Markovian Agents Models for Wireless Sensor Networks Deployed in Environmental Protection

Davide Cerotti[a], Marco Gribaudo[a], Andrea Bobbio[b]

[a]*Dipartimento di Elettronica e Informazione Politecnico di Milano, Italy, {davide.cerotti,marco.gribaudo}@polimi.it*
[b]*DiSit, Università del Piemonte Orientale, Alessandria, Italy, andrea.bobbio@unipmn.it*

Abstract

Wireless Sensor Networks (WSN) are distributed interacting systems formed by many similar tiny sensors communicating to gather information from the environment and transmit it to a base station. The present paper presents an analytical modeling and analysis technique based on Markovian Agents (MAs) and discusses a very complex scenario in which a WSN is deployed in a wide open area to monitor the outbreak of a fire and send a warning signal to a base station. The model is composed by four classes of MA modeling: the fire propagation, the high temperature front propagation, the sensor nodes and the sink; and three types of messages. It is shown that, even if the overall state space of the models is huge, nevertheless an analytical solution is feasible, by exploiting the locality of the interactions among MAs, based on a message passing mechanism combined with a perception function.

Keywords: Markovian Agent Model, Wireless Sensor Network, Fire Protection System

1. Introduction

Wireless Sensor Network (WSN) technology is becoming increasingly popular, and has been applied to a variety of monitoring and tracking applications [1]. A WSN consists of a number of sensor nodes working together to monitor the region over which they are deployed to gather data about the environment and transmit them to a central base station. In particular, WSN have witnessed a number of applications in long-duration large-scale environmental protection systems in harsh terrain, wilderness areas and location that are difficult to access [2]. Experimented application fields include environmental monitoring [2, 3], early fire detection [4, 5, 6], disaster management [7, 8], ambient air and pollution monitoring [9, 10], earthquake [11] and other vibrational phenomena [12, 11]. Among the advantages WSNs require a low micro power level, thus can last for long periods of time and have, usually, little or no infrastructure. To further save energy, nodes may undergo cycles of dormant/active periods. The main limitation is low data rate (narrower bandwidth) suitable for low data transmission applications and the reliability level of the sensor node and of the message transmission mechanisms mainly when multi-hop communication is required, due to internal failures or the exhaustion of the power source. WSNs devoted to environmental monitoring and protection are usually formed by several sensor nodes deployed in, possibly, wide geographical areas with one or more sink nodes to collect the messages transmitted by the sensing nodes. From a modeling and analysis perspective WSNs are highly distributed systems, sensitive to the geographical location, to the local conditions and to the mutual positions of the nodes. Due to these characteristics, simulation has been the prevalent analysis technique as surveyed in [13].

In recent years, a new versatile analytical technique has emerged whose main idea is to model a distributed system by means of interacting agents, so that each agent maintains its local properties but at the same time modifies its behaviour according to the influence of the interaction with the other agents. In this way, the analysis of each agent alone incorporates the effect of the interdependen-

cies. In the present model each agent selects its actions based on the current state and is represented by a continuous time Markov chain (CTMC). We refer to this kind of agents as Markovian Agents (MA) [14, 15, 16] for which the infinitesimal generator has a fixed local component, that may depend on the geographical position of the MA, and a component that depends on the interactions with other MAs. In this paper, the interaction among MAs is represented by a message passing model combined with a perception function. Different interaction mechanism are possible depending on the specific application [17].

Messages may represent either real physical messages (as in WSNs) or the mutual influences of a MA over the other MAs. The perception function regulates the propagation of messages and takes into account the MA position, the routing policy and the transmittance of the medium. Markovian Agent Models (MAMs) have proved to be suited to model and analyze very large stochastic systems of interacting heterogeneous objects, for which the dimension of the state space exceeds the capabilities of any state-space model. In the context of WSNs [14], sensor and sink nodes are represented by MAs of different classes. Nodes exchange messages whose transmission range may be very limited and may be dependent on the properties of the transmission medium; further, messages may be blocked by obstacles interposed on their passage.

In the present paper we describe a MAM modeling a WSN devoted to monitoring and protecting an outdoor environment from fire. The MAM model is composed by two interacting sub-models. The first one is inspired by a preliminary study [6] and is composed by two classes of MAs: the "fire" MA and the "Critical Temperature" MA, and models the propagation of the fire and of the front of a critical temperature. The second one is composed by two classes of MAs: the "sensor" node MA and the "central base station MA" and models the monitoring WSN, in which sensor nodes react when reached by the critical temperature front and send a warning message to the central base station, until they are eventually destroyed by the arrival of the fire. We discuss the layout of the system, how the system is sensitive to the local properties of the medium and to the presence of a non-homogeneous wind field in the area, and we study the system performance under various scenarios. We discuss the complexity of the model solution showing how the MAM model can cope, with exceptionally large state spaces.

The paper is organized as follows. Section 2 defines the Markovian Agent Model, the message emission and perception mechanism and how to construct an analytical solution. Section 3 introduces the case study and the performance measures that are computed to characterize its behaviour. Section 4 illustrates the experiments and reports the numerical results. Section 5 discusses the computational complexity of the solution and the capability of the MAM to represent environmental protection systems. Section 6 concludes the paper.

2. Theory

The Markovian Agent Model (MAM) represents a system as a collection of *Markovian Agents* (MAs) spread over a geographical space $\mathcal{V}$. The essence of the MAM is that each MA is described by a continuous time Markov chain (CTMC), whose infinitesimal generator contains a fixed component that depends on the MA structure and position in space $\mathbf{v} \in \mathcal{V}$, and a component that depends on the interaction with the other MAs.

More formally, let us call $\mathcal{V} = \{\mathbf{v_1}, \mathbf{v_2}, \ldots \mathbf{v_N}\}$ the discrete set of locations and $\boldsymbol{\pi}(t, \mathbf{v})$ the probability vector representing the state distribution of a MA at time t in position $\mathbf{v}$. Moreover, let $\Pi_{\mathcal{V}}(t)$ be the ensemble of the probability distribution of all the agents at time t. The dynamics of the probability distribution of an agent in position $\mathbf{v}$ is described by the following abstract equation:

$$\frac{d\boldsymbol{\pi}(t, \mathbf{v})}{dt} = \boldsymbol{\pi}(t, \mathbf{v})(\mathbf{Q}(\mathbf{v}) + \mathcal{I}(\mathbf{v}, \Pi_{\mathcal{V}}(t))), \qquad (1)$$

Matrix $\mathbf{Q}(\mathbf{v})$ in Equation (1) defines only the rate of local transitions, as in traditional CTMC, according to the agent position $\mathbf{v}$. The influence matrix $\mathcal{I}(\mathbf{v}, \Pi_{\mathcal{V}}(t))$ accounts for the rate of induced transitions due to the influence of other agents. The entries of matrix $\mathcal{I}(\mathbf{v}, \Pi_{\mathcal{V}}(t))$ depend on the state probabilities of other agents and must satisfy precise structural restrictions so that the matrix $\mathbf{Q}(\mathbf{v}) + \mathcal{I}(\mathbf{v}, \Pi_{\mathcal{V}}(t))$ is still an infinitesimal generator matrix. Equation (1) provides an abstract description of the agents' behaviour, since the rates of induced transitions composing the influence matrix are not fully specified. The way in which the influence matrix is defined and evaluated depends on the considered problem. In the present paper the interaction among MAs is based on a message passing mechanism combined with a perception function.

2.1. Message passing based Model

The influence among MAs is represented by the exchange of relational entities, called *messages*, that are emitted by a MA and perceived by the other ones modifying their stochastic dynamics. The interaction among agents is ruled by a *perception function* that captures the sending and receiving aptitude of the involved MAs and is a function of their geographical location and of the features of the traversed media. MAs may belong to different classes with different local behaviors and interaction capabilities, and messages may belong to different types where each type induces a different effect on the interaction mechanism. The perception function describes how a message of a given type emitted by an MA of a given class in a given position in the space is perceived by an MA of a given class in a different position.

Formally a *Multiple Agent Class, Multiple Message Type* Markovian Agents Model (M^3AM) is defined as:

$$M^3AM = \{C, \mathcal{M}, \mathcal{V}, \mathcal{U}\}, \tag{2}$$

where:

C is the set of agent classes. We denote with MA^c an agent of class $c \in C$.

$\mathcal{M}$ is the set of message types. Each agent (independently of its class) can send or receive messages of type $m \in \mathcal{M}$.

$\mathcal{V}$ is the finite (two-dimensional) space over which Markovian Agents are spread. Space $\mathcal{V}$ is discretized with a rectangular grid of $L = \ell_h \times \ell_w$ square cells of size d. From now on, the node location $\mathbf{v} = (h, w)$ identifies a discrete cell in position $h \in \{1, \ldots, \ell_h\}$ and $w \in \{1, \ldots, \ell_w\}$.

$\mathcal{U} = \{u_1(\cdot) \ldots u_M(\cdot)\}$ is a set of M perception functions, one for each message type.

Each agent MA^c of class c is characterized by a state space with n_c states, and it is defined by a tuple that depends on the particular position $\mathbf{v}$ in which the MA is located:

$$MA^c = \{\mathbf{Q^c}(\mathbf{v}), \mathbf{\Lambda}^c(\mathbf{v}), \mathbf{G}^c(\mathbf{v}, m), \mathbf{A}^c(\mathbf{v}, m), \boldsymbol{\pi}_0^c(\mathbf{v})\}. \tag{3}$$

where:

$\mathbf{Q^c}(\mathbf{v})$ is the $n_c \times n_c$ infinitesimal generator matrix of the CTMC that describes the local behavior of a class c agent in position $\mathbf{v}$.

$\mathbf{\Lambda}^c(\mathbf{v})$ is a vector of size n_c whose components represent the rates of *self-jumps* for a class c agent in position $\mathbf{v}$, i.e. the rates at which the CTMC reenters the same state.

$\mathbf{G}^c(\mathbf{v}, m)$ is a $n_c \times n_c$ matrix describing the probability that an agent of class c in position $\mathbf{v}$ generates a message of type m during a jump from state i to state j.

$\mathbf{A}^c(\mathbf{v}, m)$ is a $n_c \times n_c$ matrix, that describes the action activated upon acceptance of a type m message for an agent of class c in position $\mathbf{v}$.

$\boldsymbol{\pi}_0^c(\mathbf{v})$ is the initial state probability vector of size n_c of an agent of class c in position $\mathbf{v}$.

The perception function $u_m(\mathbf{v}, c, i, \mathbf{v}', c', i') \in [0, +\infty)$ represents the aptitude with which an agent of class c, in position $\mathbf{v}$, and in state i, perceives a message of type m generated by an agent of class c' in position $\mathbf{v}'$ in state i'.

Note that the message-based interaction paradigm, that requires the definition of a perception function, is not the only way to define Markovian Agents Models. For instance, in [17] an induction based interaction, where each agent simply "sees" the states of the neighbor agents to decide its behavior, is used to model technology switching in heterogeneous wireless communication networks (the ability to either connect to the Internet via WiFi or cellular 4G LTE).

In [18], the well known ACO (Ant Colony Optimization) model [19] is represented via MAMs by considering an extended perception function, which allows a message (modeling an ant) to be directed towards the path with the highest mean pheromone level.

2.2. Analysis

Analyzing a M^3AM consists in solving, for each MA, the differential equation for the state probability vector $\boldsymbol{\pi}^c(t, \mathbf{v}) = [\pi_i^c(t, \mathbf{v})]$, whose entries denote the probability of finding a class c agent at time t in position $\mathbf{v}$ in state i. Since $\boldsymbol{\pi}^c(t, \mathbf{v})$ is a probability vector:

$$\sum_i \pi_i^c(t, \mathbf{v}) = 1, \qquad \forall t, \forall \mathbf{v}, \forall c$$

The construction of the differential equation for $\boldsymbol{\pi}^c(t, \mathbf{v})$ requires the preliminary computation of the interactions terms. We start by defining $\beta_j^c(\mathbf{v}, m)$ as the total rate at which messages of type m are generated by an agent of

class c in state j and in position $\mathbf{v}$:

$$\beta_j^c(\mathbf{v},m) = \underbrace{\lambda_j^c(\mathbf{v})\, g_{jj}^c(\mathbf{v},m)}_{\text{ⓐ}} + \underbrace{\sum_{k\neq j} q_{jk}^c(\mathbf{v})\, g_{jk}^c(\mathbf{v},m)}_{\text{ⓑ}}. \quad (4)$$

where the first term (a) in the r.h.s is the contribution of the messages of type m emitted during a self-loop from state j and the second term (b) is the contribution of messages of type m emitted during a transition from state j to any state $k\,(\neq j)$.

The next step is to compute $\gamma_{ii}^c(t,\mathbf{v},m)$ the total rate at which messages of type m coming from the whole volume $\mathcal{V}$ are perceived by an agent of class c, in state i, in position $\mathbf{v}$, at time t.

$$\gamma_{ii}^c(t,\mathbf{v},m) = \sum_{\substack{\mathbf{v}'\in\mathcal{V}\\ \mathbf{v}'\neq\mathbf{v}}} \sum_{c'=1}^{C} \sum_{j=1}^{n_{c'}} u_m(\mathbf{v},c,i,\mathbf{v}',c',j)\,\beta_j^{c'}(\mathbf{v}',m)\,\pi_j^{c'}(t,\mathbf{v}') \quad (5)$$

The term $u_m(\mathbf{v},c,i,\mathbf{v}',c',j)\,\beta_j^{c'}(\mathbf{v}',m)\,\pi_j^{c'}(t,\mathbf{v}')$ in (5) is the rate of messages received by class c agent in state i in position $\mathbf{v}$, coming from a c' agent in position $\mathbf{v}'$ in state j, at time t. The total rate $\gamma_{ii}^c(t,\mathbf{v},m)$ is obtained summing up the contributions coming from all the states and all the agent classes, and over the entire area $\mathcal{V}$. We collect the rates (5) in a diagonal matrix $\mathbf{\Gamma}^c(t,\mathbf{v},m) = \mathrm{diag}(\gamma_{ii}^c(t,\mathbf{v},m))$. This matrix can be used to compute $\mathbf{K}^c(t,\mathbf{v})$, the infinitesimal generator of a class c agent at position $\mathbf{v}$ at time t:

$$\mathbf{K}^c(t,\mathbf{v}) = \mathbf{Q}^c(\mathbf{v}) + \sum_m \mathbf{\Gamma}^c(t,\mathbf{v},m)\,(\mathbf{A}^c(\mathbf{v},m) - \mathbf{I}) \quad (6)$$

Comparing (6) with (1), we can recognize $\mathbf{Q}^c(\mathbf{v})$ as the local transition rate matrix and the term $\sum_m \mathbf{\Gamma}^c(t,\mathbf{v},m)\,(\mathbf{A}^c(\mathbf{v},m) - \mathbf{I})$ as the definition of the influence matrix $\mathcal{I}(\mathbf{v},\Pi_{\mathcal{V}}(t))$, in this case.

The evolution of the entire model is studied by solving, separately for each MA, the following Chapman-Kolmogorov equation that incorporates the interdependency in the influence dependent component of matrix $\mathbf{K}^c(t,\mathbf{v})$.

$$\begin{cases} \boldsymbol{\pi}^c(0,\mathbf{v}) &= \boldsymbol{\pi}_0^c \\ \dfrac{d\boldsymbol{\pi}^c(t,\mathbf{v})}{dt} &= \boldsymbol{\pi}^c(t,\mathbf{v})\,\mathbf{K}^c(t,\mathbf{v}) \end{cases} \quad (7)$$

3. Model Construction

We define a M^3AM to model and analyze a complex scenario of a WSN deployed to monitor the environment from the propagation of a fire and to timely report an alarm signal to a base station. The model considers the propagation of a fire in a non-homogeneous environment, subject to a varying wind field. The front of the fire is preceded by a faster front of a high critical temperature. When the sensors scattered in the environment are reached by the temperature front they react by sending an alarm message to a base station. As the sensors are reached by the fire front they are destroyed. The M^3AM consists of four classes of MAs denoted by the superscript $C = \{f,\ h,\ s,\ b\}$ and of three types of messages denoted by $(m_f,\ m_h,\ m_w)$. MAs of classes f and h model the propagation of the fire and of the critical temperature, respectively, through the emission and perception of messages of type m_f and m_h. MAs of class s are the sensors that react to the perception of messages of type m_f and m_h and send warning messages of type m_w to the base stations MAs of class b.

In the present scenario, we assume that the geographical area of the model defined in Section 2.1 can be obtained from a satellite image like the one presented in Figure 1(a). The area is divided in $L = \ell^2$ equal square cells as in Figure 1(b) (solid line) where the dimension d of each cell is chosen in such a way that the properties of the burning material can be considered homogeneous in each cell. For the study of the fire and temperature propagation phenomenon we locate one MA^f and one MA^h per cell, so that there are L MAs of class f and L MAs of class h. In the present experiment, the sensor nodes of class MA^s are distributed regularly on the area $\mathcal{V}$ at a distance compatible with the transmission range of each sensor. We locate one sensor node every w cells of the grid, so that there are in total $L_w = \ell^2/w^2$ sensor nodes MA^s in the area, as shown in the dashed grid of Figure 1(b). Finally, we locate only one base station MA^b at one corner of the area $\mathcal{V}$ (Figure 1(b)). In the pictorial representation of a MA, the local transitions (pertaining to matrix $\mathbf{Q}^c(\mathbf{v})$) are depicted in solid line and are labeled with the corresponding entry of matrix $\mathbf{Q}^c(\mathbf{v})$, while induced transitions (pertaining to matrix $\Gamma^c(t,\mathbf{v},m)$) are depicted in dashed line and are labeled with the type of message whose perception induces the transition.

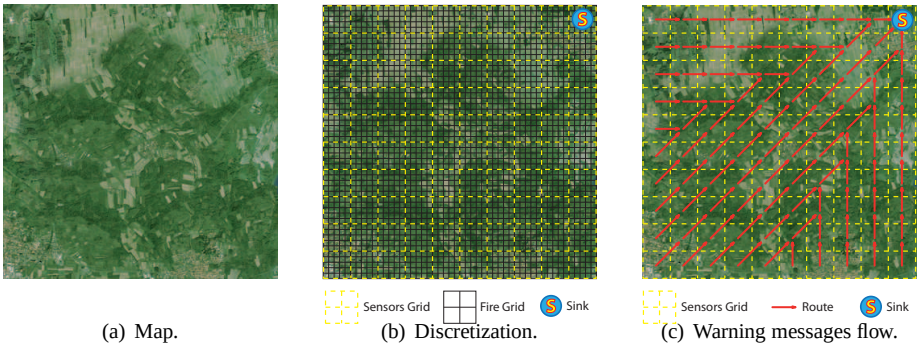

(a) Map. (b) Discretization. (c) Warning messages flow.

Figure 1: A aerial view of the area of the experiment: a) the map; b) the fire and temperature grid (solid line 50×50 cells) and the sensor grid (dashed line 10×10 cells); c) the superimposed routing table.

3.1. MA for fire and temperature propagation front

The fire and temperature propagation dynamics in outdoor environments depends on several factors such as the density and type of materials being incinerated, the wind direction, etc. In a homogeneous environment and in the absence of wind, the flame front spreads circularly, while in the presence of wind it spreads following an ellipse with main axis in the direction of the wind [6]. The propagation model should account for the flame front and the critical temperature front. The class of the fire MA^f has three states (I, B, E) and can emit two types of messages (m_f, m_h) and is reported in Figure 2a). The meaning of the states is the following:

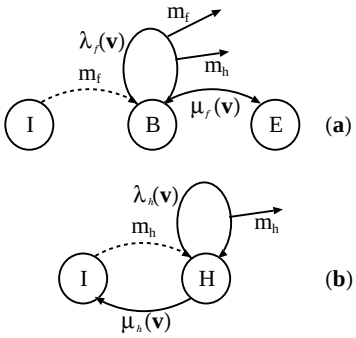

Figure 2: Fire Agent MA^f (a) and Temperature Agent MA^h (b)

I - is the idle state: the cell is not burning. When a fire message m_f arrives, an induced transition (dashed line) makes the MA jump to the burning state B.

B - is the burning state: the cell is reached by the fire front. When resident in state B two local transitions are possible (solid line). With rate $\lambda_f(\mathbf{v})$ the MA broadcasts two types of messages m_f and m_h, with probability 1. The value of $\lambda_f(\mathbf{v})$ determines the frequency at which messages are emitted and hence, the speed at which the fire front propagates; further, since its value depends on $\mathbf{v}$, we can assign a different propagation rate to each cell thus modeling a non-homogeneous terrain. The rate $\mu_f(\mathbf{v})$ is instead the extinguishing rate. When the corresponding transition fires, the MA jumps to the extinguished state E which acts as an absorbing state. Also in this case the parameter value depends on $\mathbf{v}$ so that the time to extinction of the fire may be related to the local properties of the terrain in the cell.

E - is the extinguished state: the fire is extinguished and the activity of the MA^f terminates.

The class of the MA^h temperature agents has two states (I, H) and can emit one type of message (m_h), as shown in Figure 2b). The meaning of the states is the following:

I - is the idle state: the cell is below the critical temperature. When a temperature message m_h is perceived, the agent jumps to state H.

H - is the critical temperature state: the cell is reached by the critical temperature front. When resident in H two local transitions are possible (solid line). With rate $\lambda_h(\mathbf{v})$ the MA broadcasts a message of type m_h, and the value of $\lambda_h(\mathbf{v})$ determines the speed at which

the temperature front propagates. With rate $\mu_h(\mathbf{v})$ the agent becomes idle again.

The elliptic propagation model of either fire or temperature front, is determined by two perception functions u_{m_h} and u_{m_f}. A MA^f in position $\mathbf{v}$ perceives fire messages from MA^fs in position $\mathbf{v}'$, only if the distance between the two agents is inside the propagation ellipse centered on the position $\mathbf{v}'$ of the sender agent. Moreover, it receives such messages at a rate proportional to the distance R_f from the originating focus. In this way, the front propagation is governed by the interaction among cells inside the propagation ellipse.

$$u_{m_f}(\mathbf{v}, f, i, \mathbf{v}', f', j) = \begin{cases} R_f & \text{if } (\mathbf{v}' - \mathbf{v}) \leq min(R_f, 1)) \\ & \wedge\, (i = I) \wedge (j = B) \\ 0 & \text{otherwise} \end{cases} \tag{8}$$

where, R_f is the equation in polar coordinates (R, θ) of an ellipse with semi-major axis of length a_f, eccentricity ϵ_f and rotation angle α_f, and is given by:

$$R_f = \frac{a_f(1 - \epsilon_f^2)}{1 - \epsilon_f\, Cos(\theta - \alpha)} \tag{9}$$

The eccentricity ϵ_f depends on the wind speed W, and the rotation angle α_f on the wind direction [6]. The perception function $u_{m_h}(\mathbf{v}, t, i, \mathbf{v}', t', j)$ for the temperature message m_h is constructed in a similar way, by defining the corresponding propagation ellipse R_h as in Equation (9), with parameters a_h and ϵ_h, and replacing this value in Equation (8). In this case, messages are emitted by either a MA_f in state B or a MA_h is state H and perceived by a MA_h in state I.

3.2. MA for the sensor network

The WSN in charge of fire monitoring is composed by regularly spaced sensor nodes of class MA^s as shown in Figure 1b). When one sensor is reached by the temperature front it starts sending warning messages of type m_w toward the sink. To preserve the battery, messages have a limited transmission range and are sent to neighboring sensors according to a predefined routing protocol so that the warning messages reach the base station through a multi-hop mechanism. To further preserve energy, nodes undergo cycles of dormant/active periods, so that they can sense and transmit messages only when active. Sensors are destroyed when reached by the fire front. The WSN is modeled by two MA classes: the *sensor node* class MA^s and the *sink node* class MA^b. They interact with the fire and temperature agents MA^f and MA^h by means of messages m_f, m_h. The agent of class MA^s is characterized by

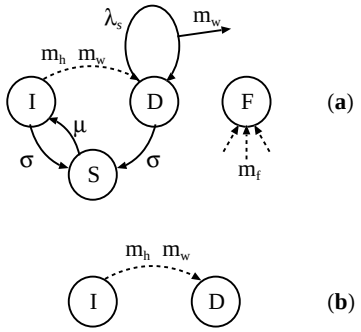

Figure 3: Sensor Agent MA^s(a) and Base Station Agent MA^b (b) . The dangling arrows directed to fail state F represent that from any state the reception of m_f messages induce a transition to F.

4 states and can perceive 3 types of messages (m_h, m_f, m_w) but can emit only messages of type m_w. MA^s is depicted in Figure 3(a). The meaning of the states is the following:

- I - is the idle state: the sensor is quiet until it perceives a temperature message m_h or a warning message m_w. The idle state alternates with the sleeping state S where the sensor is inactive.
- D - is the detection state: the node has detected either a message m_h or m_w and propagates the warning message m_w at a rate λ_s according to a given routing table.
- S - is the sleeping state: the radio device and sensing equipment are switched off; the wake up transition of rate μ is always to state I.
- F - is the fail (absorbing) state and is reached when the sensor is stricken by the fire front.

The behavior of the MA^s agent at the reception of the messages is the following:

- the reception of m_h in state I induces a transition to state D with probability 1.
- the reception of m_f in states I, D or S induces a transition to state F with probability 1.

- the reception of a warning message m_w in state I activates the sensor to state D with probability 1 where the warning message m_w is replicated with rate λ_s.

A sensor node can go to sleep (in state S) either from I or D with rate σ and wakes up at rate μ. When a sensor goes to sleep from state D it forgets any previous incoming signal and returns active always in state I.

The base station agent MA^b has a simple structure, characterized by an idle state I and a detection state D and is depicted in Figure 3b); MA^b is not destroyed by the fire and the transition from I to D occurs at the reception of the temperature message m_h or the warning message m_w. In our experiments there is only one base station located in one corner of the grid (Figure 1).

To speed up the alert and save energy, each sensor sends the warning messages to its first neighbor in the direction of the sink according to a predefined routing table whose visual representation is reported in Figure 1c). The flow of messages is indicated by arrows. We define the routing table function $\mathcal{RT}(\mathbf{v}, \mathbf{v}') = 1$, when a MA^s in position $\mathbf{v}$ is directly connected to a first neighbor MA^s in position $\mathbf{v}'$ by an arrow in the routing flow diagram of Figure 1c); $\mathcal{RT}(\mathbf{v}, \mathbf{v}') = 0$, otherwise. Given the routing table, the perception function for the warning message m_w is defined as:

$$u_{m_w}(\mathbf{v}, t, i, \mathbf{v}', t', j) = \begin{cases} 1 & \text{if } \mathcal{RT}(\mathbf{v}', \mathbf{v}) = 1 \wedge \\ & i = I \wedge j = D \\ 0 & \text{otherwise} \end{cases} \quad (10)$$

The interactions between an MA^f and an MA^s by means of messages m_f and between an MA^h and an MA^s (or MA^b) by means of messages m_h are defined according to the perception functions $u_{m_f}(\cdot)$ and $u_{m_h}(\cdot)$ described by Equations (8).

3.3. Performance indexes

Solving a M^3AM means computing the probability vector $\boldsymbol{\pi}^c(t, \mathbf{v})$ as a function of time t for every MA present in the area $\mathcal{V}$ by means of an equation of type (7). The knowledge of the $\boldsymbol{\pi}^c(t, \mathbf{v})$ provides a complete description of the model and allows us to compute various performance measures of interest.

Fire and temperature propagation front - The spatial propagation of the fire front is given by the spatial probability $\pi^f_B(t, \mathbf{v})$ of the agents MA^f of being in the burning state B. Similarly for the propagation of the temperature front.

Mean Fire Propagation Time - The Mean Fire Propagation Time $\eta^f(\mathbf{v}, \mathbf{v}')$ is the mean time needed by the fire to reach a cell in position $\mathbf{v}'$ starting from a cell in position $\mathbf{v}$. $\eta^f(\mathbf{v}, \mathbf{v}')$ is computed by taking the expectation of the random variable $\Omega(\mathbf{v}, \mathbf{v}')$ representing the first passage time from $\mathbf{v}$ to $\mathbf{v}'$ that in turn is computed starting the fire in the MA^f in position $\mathbf{v}$ and by making absorbing the MA^f in position $\mathbf{v}'$. To compute $\eta^f(\mathbf{v}, \mathbf{v}')$ we perform the transient analysis by assuming as initial conditions that the MA^f in position $\mathbf{v}$ is in state B (burning) with probability 1 and all the other MA^fs are in state I (idle):

$$\pi^f_i(0, \phi) = \begin{cases} 1 & \text{if } ((\phi = \mathbf{v}) \wedge i = B) \vee \\ & (\phi \neq \mathbf{v}) \wedge i = I)) \\ 0 & \text{otherwise} \end{cases}$$

where ϕ is a generic position that spans over $\mathcal{V}$ and i a generic state. Further the burning state B of the MA^f in position $\mathbf{v}'$ is changed to an *absorbing state*. From standard probability theory results (see [20]) we have that the Cumulative Distribution Function of $\Omega(\mathbf{v}, \mathbf{v}')$ is given by:

$$Pr(\Omega(\mathbf{v}, \mathbf{v}') \leq t) = \pi^f_B(t, \mathbf{v}')$$

$$\eta^f(\mathbf{v}, \mathbf{v}') = E[\Omega(\mathbf{v}, \mathbf{v}')] = \int_0^{+\infty} (1 - \pi^f_B(t, \mathbf{v}'))\, dt \quad (11)$$

Mean Message Travel Time - In an similar way, we can compute the mean travel time $\eta^w(\mathbf{v}, \mathbf{v}')$ needed by a message m_w originated from a MA^s in position $\mathbf{v}$ to reach in a multi-hop path a MA^s in position $\mathbf{v}'$. In particular we investigate $\eta^w(\mathbf{v}, \mathbf{v_b})$, the mean travel time taken by a message m_w to reach the sink. This measure provides an index of the "responsiveness" of the WSN in terms of how quickly the network can deliver early warning messages to the sink, before fire arrives.

4. Experiments and Results

All the experiments were performed in the geographical area shown in Figure 1a) with a square grid of $L = 50 \times 50$ cells numbered in the standard Cartesian way. Cell $(0, 0)$ is at the left bottom corner and cell $(50, 50)$ at the right top corner. We locate one MA^f and one MA^h per cell. The parameters of the agents can be automatically

extracted from the RGB coding of the aerial image of the map through an Adobe Flash application as reported in [6]. At time $t = 0$ all the agents are in their idle state I with probability 1 ($\pi_I^f(0, \mathbf{v}) = \pi_I^h(0, \mathbf{v}) = 1 \ \ \forall \mathbf{v}$). To start a fire in location ϕ at $t = 0$ we assign an initial probability equal to 1 to the burning state B of the MA^f in the given location: $\pi_B^f(0, \phi) = 1$. The analysis is ccarried out by solving the differential Equations (7) using the TR-BDF2 technique [21]. The computations time ranges from five to ten minutes on a notebook equipped with an Intel Core i5 CPU at 2.5 GHz.x 4 and 5.8GB RAM.

4.1. Fire and Temperature Propagation Front

This Section analyses the dynamic behaviour of the fire and temperature propagation front in an open environment in the presence of obstacles. In the area of Figure 1a) we have located a lake that acts as a barrier preventing the fire to propagate (Figure 4). To model the obstacle, the agents in the cells covered by the lake are removed. The message emission rates of both MA^f and MA^h are constant with $\lambda_f(\mathbf{v}) = 0.1 \ min^{-1}$ and $\lambda_h(\mathbf{v}) = 0.2 \ min^{-1} \ \ \forall \mathbf{v}$, respectively. The extinguishing rates are the same for both agents in each cell $\mu_f(\mathbf{v}) = \mu_h(\mathbf{v})$ but vary from cell to cell in the range $(0 - 0.05)$ since they are automatically extracted from the map.

We focus on the spatial distribution of the probability $\pi_B^f(t, \mathbf{v})$ of the MA^f in the burning state B and of the probability $\pi_H^h(t, \mathbf{v})$ of the MA^h in the critical temperature state H. We plot such values in a colored map: darker points in the grid correspond to low probability values, while lighter points indicate higher values. To provide a better visual distinction between the fire and the temperature front, we have plotted for the former only probability values in the range $0.7 \leq \pi_B^f(t, \mathbf{v}) \leq 0.9$ (corresponding to yellow color) and for the latter values in the range $0.6 \leq \pi_H^h(t, \mathbf{v}) \leq 0.8$ (corresponding to pink color). We study the propagation in two different environmental conditions: a wind blowing with a constant low speed in a fixed direction from west to east (Figures 4(a-d)) and a wind at high speed with a constant direction from north to south (Figures 4(e-h)). In both conditions, the fire originates at position $\mathbf{v_f} = (0, 49)$, and the dynamic of the front propagation is plotted at the time instants $t = 5, \ 10, \ 15, \ 20 \ min$.

Figures 4(a-d) show the propagation with light wind: at minute 5 the initial temperature front in the upper left corner of the image is just visible; at minute 10 the temperature front reaches the lake, and the fire becomes visible in the upper left corner. Proceeding with time, the lake divides the temperature front in two parts and the fire grows covering a larger zone as clearly visible at minute 15. Finally at minute 20, the temperature front exits from the map and the fire propagation is hindered by the lake.

With a strong wind the propagation is significantly quicker and with a different dynamic as shown in Figures 4(e-h). At minute 5 the temperature front reaches the west side and surpasses the east side of the lake, while the fire is still in the corner. At minute 10 the fire reaches the lake and the temperature front is already beyond the map. Also in this case the fire is hindered by the lake, but the wind is strong enough to let the fire circumvent the lake as shown at minute 15. From now on the fire is free to spread beyond the lake and to cover a significant part of the whole area (minute 20). Finally, we have supposed that there is a critical structure (a house, a village) in the left lower corner of the map at the cell $\mathbf{v_{crit}} = (0, 0)$ and we have measured the mean time $\eta^f(\mathbf{v_f}, \mathbf{v_{crit}})$ needed by the fire to reach the critical location. With a light wind $\eta^f(\mathbf{v_f}, \mathbf{v_{crit}})$ is about 39 *min*, whereas with a strong south directed wind it is reduced to about 17 *min*.

4.2. WSN analysis

This Section is dedicated to analyse the WSN in isolation, i.e. without considering its interaction with the temperature and fire agents. This analysis is intended to be useful in a preliminary design phase to tune the structure and the parameters of the WSN. The parameters that influence the performance of the WSN are, primarily, the distance w (measured in number of cells), the sending rate of warning messages λ_s and the duration of the sleeping cycle α of active-sleeping periods determined by the values of the rates σ and μ:

$$\alpha = 100 \, \frac{\sigma}{\sigma + \mu} \tag{12}$$

The experiments have been performed considering the geographical area of Figure 1b) in which the MA^s sensor agents are located at the intersection of the dashed grid with step w and one single sink agent MA^b is always located in a fixed position $\mathbf{v_b} = (48, 48)$. The analysis is concentrated to find the average travel time of the warning message $\eta^w(\mathbf{v_a}, \mathbf{v_b})$ from a given position $\mathbf{v_a}$ to the sink

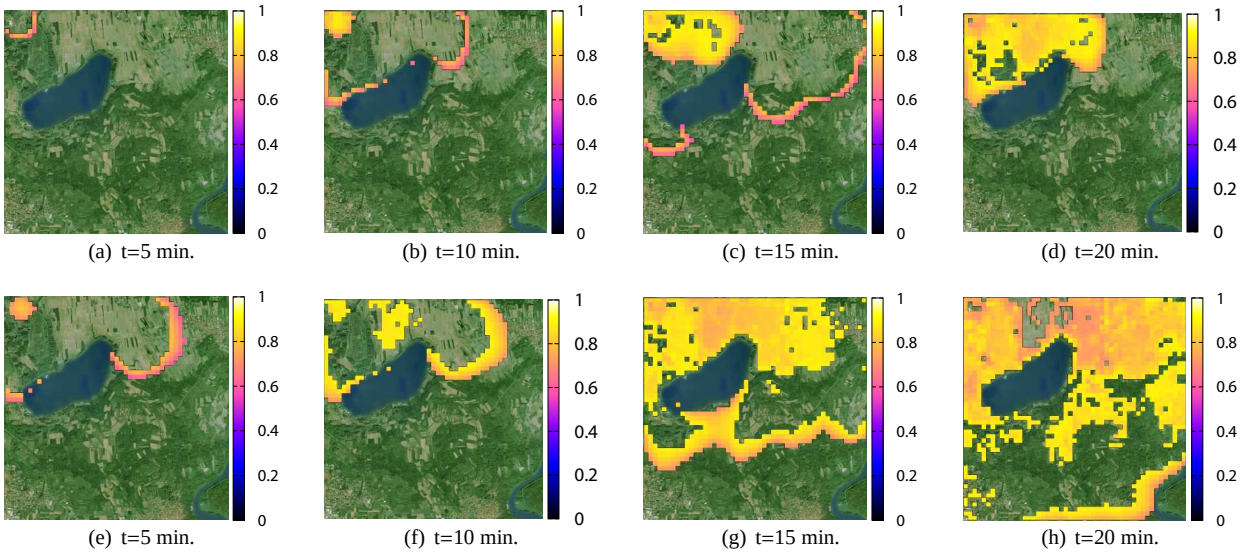

(a) t=5 min. (b) t=10 min. (c) t=15 min. (d) t=20 min.

(e) t=5 min. (f) t=10 min. (g) t=15 min. (h) t=20 min.

Figure 4: Fire and temperature propagation front in the presence of an obstacle

$\mathbf{v_b}$, as a function of the position $\mathbf{v_a}$, of the sleeping cycle α and of the distance w. To generate the warning signal, at time $t = 0$ the single sensor in position $\mathbf{v_a}$ is made active in the detection state D by setting $\pi^s_D(0, \mathbf{v_a}) = 1$, and remains active so that for the duration of the entire experiment it emits warning messages m_w at rate λ_s. All the others MA^s agents follow the same sleeping-active cycles with sleeping cycle α and are assigned an initial probability $\pi^s_I(0, \mathbf{v}) = 1 - \alpha$ and $\pi^s_S(0, \mathbf{v}) = \alpha$ for all $\mathbf{v} \neq \mathbf{v_a}$.

In the experiments we have considered a set of positions $\mathbf{v_a} = \{(0, 0), (24, 24), (36, 36)\}$, two values of the sending rate $\lambda_s = \{1.667, 0.2\}$ sec^{-1} (corresponding to a mean time between message emissions of 0.6 and 5 *sec*, respectively) and two sizes of the grid topology with ($w = 6$) and ($w = 12$) (to change the number of hops to reach the sink). Further, the sleeping cycle α varies in the range $[0 - 95]$. The results are shown in Figure 5. In all the experiments two effects are always visible. First, the travel time of the warning messages $\eta^w(\mathbf{v_a}, \mathbf{v_b})$ is directly proportional to the distance between the location $\mathbf{v_a}$ generating the message and the sink $\mathbf{v_b}$; second, an increment of the sleeping percentage increases the travel time since it increases the probability that at each hop a sensor wastes time sending messages to a sleeping sensor. However, such an increment depends on the network characteristics. With a high transmission rate ($\lambda_s = 1.667$ sec^{-1}) this effect becomes significant only for very high sleeping percentages (of the order of $\alpha = 90\%$) as shown in Figure 5(a-b). A stronger effect appears with a lower transmission rate of $\lambda_s = 0.2$ sec^{-1} as shown in Figure 5(c-d) where a significant increment in the mean travel time appears for lower values of α particularly in the case $w = 6$.

4.3. WSN detecting incoming fire

In this Section we combine the fire and temperature propagation model of Section 3.1 with the WSN detection and warning model of Section 3.2. The model locates one MA^f and one MA^h in each cell, and one MA^s every $w = 8$ cells. The fire propagation rate λ_f and the temperature propagation rate λ_h are constant over all the cells with $\lambda_f = 2.0$ min^{-1} and $\lambda_h = 4.0$ min^{-1}, respectively. For each cell the wind intensity is low and the direction constant. To show that the model can handle non-homogeneous and location-dependent phenomena [7], the extinction rate of both fire and temperature are automatically extracted from the colored map in Figure 1(a) so that any cell may have a different rate value. In the present set of experiments those values range from 0.2 to 0.9 min^{-1}.

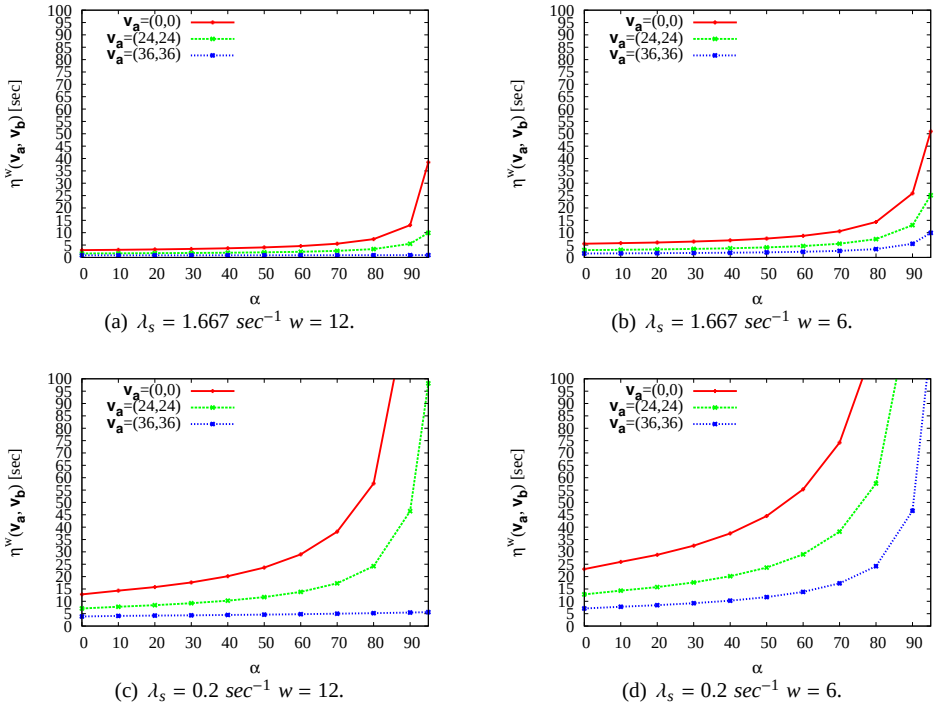

(a) $\lambda_s = 1.667\ sec^{-1}$ $w = 12$. (b) $\lambda_s = 1.667\ sec^{-1}$ $w = 6$.

(c) $\lambda_s = 0.2\ sec^{-1}$ $w = 12$. (d) $\lambda_s = 0.2\ sec^{-1}$ $w = 6$.

Figure 5: Travel time of warning messages varying the sleeping time percentage and for different always active sensor positions.

The fire starts in the left lower corner in position $\mathbf{v_f} = (0, 0)$, while the sink is located at the opposite corner in position $\mathbf{v_b} = (48, 48)$. Each sensor is tuned with a low sleeping percentage $\alpha = 20\%$. The sending rate of the warning messages is $\lambda_s = 100\ min^{-1}$, about two orders of magnitude greater than the rate of the fire propagation. In the figures the sensors are spotted as small squares.

Figures 6(a-d) show the spatial and time evolution of the probabilities of having MA^f in the burning state B, MA^h in the critical temperature state H and $MA^{s,b}$ in the detection state D. The figures capture the dynamics of the model at the time instants $t = 2,\ 5,\ 20,\ 30\ min$. As in previous experiments, to distinguish the fire and the temperature front, all the values of $0 \leq \pi^f_B(t, \mathbf{v}) \leq 1.0$ are plotted whereas for the temperature only the values $0.4 \leq \pi^h_H(t, \mathbf{v}) \leq 0.8$ are plotted in purple/blue (dark) color. For the sensors, all the values of $0 \leq \pi^s_D(t, \mathbf{v}) \leq 1.0$ are drawn on the figures. To improve the visibility of the sensors dynamics, Figures 6(e-h) isolate the spatial probability $\pi^s_D(t, \mathbf{v})$ for the sensors $MA^{s,b}$, only, and with a different color scale (from white/yellow for low probabilities to dark blue for high probabilities).

The fire spreads slowly in an approximately circular way with slight variations due to the non-homogeneous extinction rates and the light wind. Due to the high coverage of monitored area, the WSN can detect the fire almost immediately: even at $t = 2\ min$, when the fire is just started at the lower-left corner, the path of colored squares along the diagonal of the area indicates a flow of warning messages towards the sink. At $t = 5\ min$ the probability that such sensors have detected the fire is almost one. At $t = 20\ min$, other sensor routes, leading from the fire to sink, starts to appear: this can be used by the base station to monitor the extension of the fire. At $t = 30\ min$, almost all the sensors have detected the fire, that has already reached half-way to the sink. From the sensor messages, the base station can estimate the speed and extension of the fire front, and properly direct the actions of the fire-

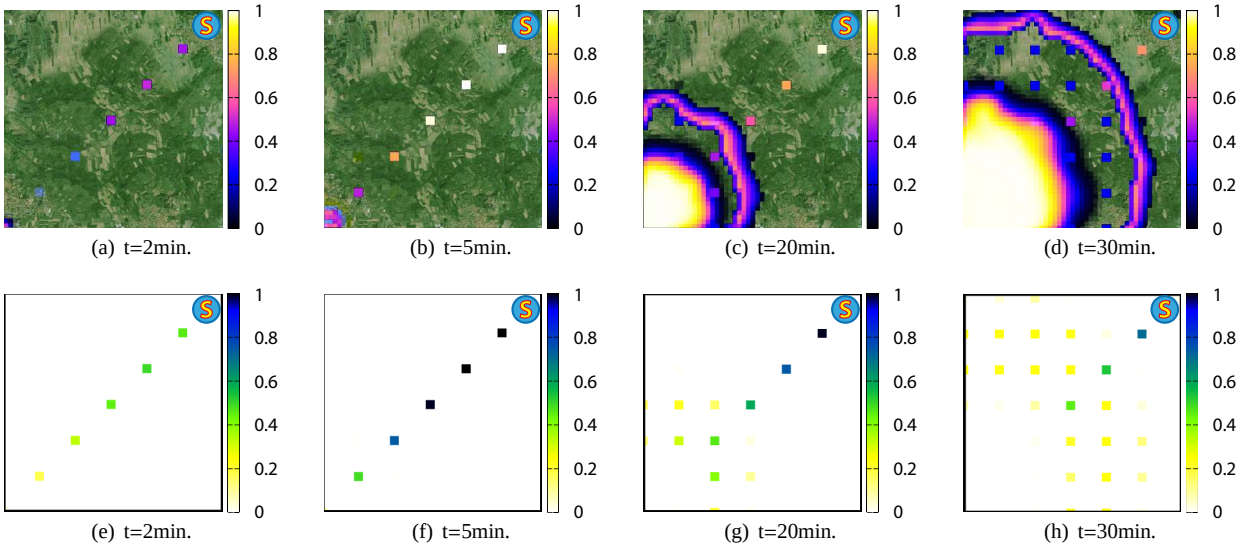

(a) t=2min. (b) t=5min. (c) t=20min. (d) t=30min.

(e) t=2min. (f) t=5min. (g) t=20min. (h) t=30min.

Figure 6: The WSN detects the incoming fire and alerts the base station.

fighters.

5. Discussion

5.1. Complexity

The state space of the example discussed in Section 4 has the following size. There are $\ell^2 = 2500$ MA^f (with 3 states) and MA^h (with 2 states). There are $(\ell/w)^2 = 64$ MA^s (with 4 states) and there is one MA^b (with 2 states). The total number of states of the model is therefore:

$$N_T = 3^{2500} \times 2^{2500} \times 4^{64} \times 2 \qquad (13)$$

which is a number that is hardly explored even by simulation. Our analytical technique is feasible since we solve separately 2500 Equations of the form (7) for MA^f, 2500 for MA^h, 64 for MA^s and 1 for MA^b. An exponential complexity is reduced to a linear complexity. However, to arrive to solve one Chapman-Kolmogorov equation of type (7) for a given agent of class c, we need to compute first the influence matrix $\mathbf{K}^c(t, \mathbf{v})$. If we denote by $n_* = Max\{n_c\}$ the largest dimension of the state space of MA of any class, the computation of matrix $\mathbf{K}^c(t, \mathbf{v})$ requires M computations of the diagonal matrix $\mathbf{\Gamma}^c(t, \mathbf{v}, m)$, one for each message type. Matrix $\mathbf{\Gamma}^c(t, \mathbf{v}, m)$ has at most n_* entries that account for all the interactions with all the MAs in the whole area $\mathcal{V}$ during sojourn in state i, (see Equation (5)). Let N_I be the number of such possible interactions; in the worst-case each MA interacts with all the other ones and hence $N_I = C\, n_* \ell^2$. In the worst-case the complexity of the computation of matrix $\mathbf{K}^c(t, \mathbf{v})$ is $O(n_*\, N_I) = O(C\, n_*^2 \ell^2)$. In the described scenario the worst-case complexity would be $O(4 \times 4^2 \times 2500) = O(160000)$.

However, and this is the main point of the technique, the worst-case complexity is greatly reduced since the interaction of each MA is often limited to a subset of message types and is confined to a restricted region around the position of the MA by means of the perception function $u(\cdot)$. In our scenario each MA^f perceives messages only of type m_f from MA^fs that are inside the propagation ellipse (as described by the perception function in (8)) that covers on the average 24 cells. MA^h perceives messages only of type m_h from MA^fs or MA^hs that are inside the same propagation ellipse. Each MA^s perceives messages of types m_f, m_h and m_w from MA^fs or MA^hs or MA^s according to the routing table indicated with arrows in Figure 1. As can be inferred from Figure 1 each MA^s perceives messages only from one or two first neighboring MA^s. Fi-

nally, the sink MA^b perceives messages of types m_h and m_w from the 3 first neighboring locations only (Figure 1). For such reasons, in our scenario the real number of interactions to be taken into account in the computation of matrix $\mathbf{K}^c(t, \mathbf{v})$ is approximately $N_{I_*} \leq 200$, with an enormous reduction in comparison with the worst-case.

The Equations (7) are solved by resorting to numerical iterative techniques over a discretized time interval. The $0 - T_W$ mission time is uniformly discretized with step Δt yielding $T_\Delta = T_W/\Delta t$ time points. Thus, in the worst-case the time complexity of the solution algorithm turns out to be $O(T_\Delta M \ell^4 C^2 n_*^2)$. In our scenario the complexity is reduced to $O(N_{I_*} T_\Delta \ell^2 C M n_*)$ since, as outlined earlier, the possible interactions of each MA with its neighbors are limited (that is, $N_{I_*} << N_I = \ell^2 C n_*$). The capability of the M^3AM to confine and localize the interactions is one of its main peculiar properties that is exploited in any practical application.

5.2. Environmental protection systems

Environmental protection systems are usually implemented with a network of Intelligent Guards against Disasters(iGaDs) devices [3] which locally maintain location information and behave according to their own position. Such feature can be naturally included in MAM models. For instance, the perception function can be used to model power decay of a message transmission depending on the relative distance between source and destination. Moreover, the work in [16] shows that MAM can also represent and evaluate distributed gradient-based routing algorithms for WSN with time-varying topology.

The ability of iGaDs network to deliver early warning depends on network parameters, such as the frequency of forwarding, the transmission range and the network topology. But it is also affected by the physical characteristics of the considered environmental threat, such as its propagation speed and its direction. Thus, a proper model should take into account both the monitoring system and the disaster dynamic to capture their interdependencies. To the best of our knowledge, such holistic approach is rarely applied. On the one hand, iGaDs are evaluated by analytic or simulative models in which the disaster event is represented by just a probability of occurrence or a rate; on the other hand, disaster dynamics are evaluated by simulation of complex model without considering the iGaDs. Instead, in this work we have shown that a unified MAM model, even with the simplified fire propagation model in Section 3.1, can provide useful insight about the iGaDs system performance.

6. Conclusions

In this work we presented a modeling technique to study, within a single unified framework, the propagation of an environmental hazard (a forest fire) together with the performance of a WSNs deployed to timely detect the hazard by sending warning messages to a base station. Despite the huge complexity of the state space of the overall model, the MAM formalism has been able to build up a set of analytical equations that are numerically tractable. The main feature of the MAM models is its ability to confine the interaction of each entity of the distributed system to a delimited environment as it is often observed in many real large-scale distributed applications. Further, the MAM model is sensitive to the position of each entity and to their relative distances so that highly non-homogeneous phenomena can be naturally captured. Along the line presented in this paper, the methodology can be refined to improve the WSN alarm protocols, to optimize the sensor placement, and to optimize the model parameters, to increase the sensor lifetime and reduce the time to detect the hazard.

However, various new directions can be envisaged to expand and improve the MAM modeling technique. Investigate more abstract interaction mechanisms not based on the message passing paradigm combined with a perception function. Include the mobility of the entities. Define a high level language to facilitate the description of the model.

References

[1] J. Yick, B. Mukherjee, D. Ghosal, Wireless sensor network survey, Computer Networks 52 (12) (2008) 2292 – 2330.

[2] P. Corke, T. Wark, R. Jurdak, W. Hu, P. Valencia, D. Moore, Environmental wireless sensor networks, Proceedings of the IEEE 98 (11) (2010) 1903–1917. URL `http://eprints.qut.edu.au/42703/`

[3] J. W. Liu, C.-S. Shih, E. T.-H. Chu, Cyberphysical elements of disaster-prepared smart environments, Computer 46 (2) (2013) 69–75.

[4] B. Son, Y. He, J. Kim, A design and implementation of forest-fires surveillance system based on wireless sensor networks for south Korea mountains, International Journal of Computer Science and Network Security 6 (9B) (2006) 124–130.

[5] J. Lloret, D. B. M.l Garcia and, S. Sendra, A wireless sensor network deployment for rural and forest fire detection and verification, Sensors 9 (2009) 8722–8747.

[6] D. Cerotti, M. Gribaudo, A. Bobbio, C. Calafate, P.Manzoni, A Markovian agent model for fire propagation in outdoor environments, in: Computer Performance Engineering (EPEW2010), Springer - LNCS, Vol 6342, 2010, pp. 131–146.

[7] A. B. D. Cerotti, M. Gribaudo, Disaster propagation in inhomogeneous media via markovian agents, in: Critical Information Infrastructure Security, Springer Verlag - LNCS, Vol 5508, 2009, pp. 328–335.

[8] M. Bahrepour, N. Meratnia, M. Poel, Z. Taghikhaki, P. Havinga, Distributed event detection in wireless sensor networks for disaster management, in: 2nd International Conference on Intelligent Networking and Collaborative Systems (INCOS), 2010, IEEE, 2010, pp. 507–512.

[9] Y. Ma, M. Richard, M. Ghanem, Y. Guo, J. Hassard, Air pollution monitoring and mining based on sensor grid in London, Sensors 8 (6) (2008) 3601–3623.

[10] K. Khedo, R. Perseedoss, A. Mungur, A wireless sensor network air pollution monitoring system, International Journal of Wireless & Mobile Networks 2 (2) (2010) 31,45.

[11] M. Suzuki, S. Saruwatar, N. Kurata, H. Morikawa, A high-density earthquake monitoring system using wireless sensor networks, in: Proceedings of the 5th international conference on Embedded networked sensor systems, SenSys '07, ACM, New York, NY, USA, 2007, pp. 373–374.

[12] G. Werner-Allen, K. Lorincz, M. Rui, O. Marcillo, J. Johnson, J. Lees, M. Welsh, Deploying a wireless sensor network on an active volcano, IEEE Internet Computing 10 (2) (2006) 18–25.

[13] F. Yu, A survey of wireless sensor network simulation tools, http://www1.cse.wustl.edu/ jain/cse567-11/ftp/sensor/index.html (2011) 1–10.

[14] M. Gribaudo, D. Cerotti, A. Bobbio, Analysis of on-off policies in sensor networks using interacting Markovian agents, in: 4-th Int Work Sensor Networks and Systems for Pervasive Computing - PerSens 2008, 2008, pp. 300–305.

[15] M. C. Guenther, J. T. Bradley, Higher moment analysis of a spatial stochastic process algebra, in: Computer Performance Engineering, Springer - LNCS, Vol 6977, Springer, 2011, pp. 87–101.

[16] D. Bruneo, M. Scarpa, A. Bobbio, D. Cerotti, M. Gribaudo, Markovian agent modeling swarm intelligence algorithms in wireless sensor networks, Performance Evaluation 69 (2012) 135–149.

[17] M. Gribaudo, D. Manini, C.-F. Chiasserini, Studying mobile internet technologies with agent based mean-field models., in: A. N. Dudin, K. D. Turck (Eds.), ASMTA, Vol. 7984 of Lecture Notes in Computer Science, Springer, 2013, pp. 112–126.

[18] D. Cerotti, M. Gribaudo, A. Bobbio, D. Bruneo, M. Scarpa, An intelligent swarm of markovian agents, Tech. rep., Politecnico di Milano, Italy, TO APPEAR.

[19] M. Dorigo, T. Stützle, Ant Colony Optimization, MIT Press, 2004.

[20] K. S. Trivedi, Probability and statistics with reliability, queuing and computer science applications, John Wiley and Sons Ltd., Chichester, UK, 2002.

[21] R. E. Bank, W. M. C. Jr., W. Fichtner, E. Grosse, D. J. Rose, R. K. Smith, Transient simulation of silicon devices and circuits, IEEE Trans. on CAD of Integrated Circuits and Systems 4 (4) (1985) 436–451.